

## Raman scattering in carbon nanotubes revisited

J. Maultzsch, S. Reich, and C. Thomsen

*Institut für Festkörperphysik, Technische Universität Berlin, Hardenbergstr. 36, 10623 Berlin, Germany*

(Received 14 March 2002; published 23 May 2002)

We explain the origin of the high-energy mode in the first-order Raman spectra of single-walled carbon nanotubes by double-resonant scattering. Following this interpretation, we calculate the multiple-peak structure as found in Raman experiments. The highest peak is above the graphite  $\Gamma$ -point frequency; its amplitude is larger than that of the second peak. We derive positive and negative frequency shifts as a function of excitation energy, which we observe experimentally as well. We predict a difference in frequency and shape of the high-energy mode in Stokes and anti-Stokes scattering.

DOI: 10.1103/PhysRevB.65.233402

PACS number(s): 78.30.Na, 63.22.+m, 71.20.Tx

Raman spectroscopy is widely used to investigate both vibrational and electronic properties of solids. Because of the small wave vector transfer in first-order scattering, only phonon modes with a nearly zero wave vector are expected in first-order Raman spectra. In particular, two of the three characteristic peaks in the first-order spectra of carbon nanotubes, the radial breathing mode at  $\approx 200 \text{ cm}^{-1}$  (Refs. 1 and 2) and the high-energy graphitelike mode at  $\approx 1600 \text{ cm}^{-1}$ , have so far been implicitly assumed to be  $\Gamma$ -point modes. Most conclusions derived from Raman experiments are based on the  $\Gamma$ -point nature of these modes, e.g., an experimental determination of the tube diameter, chirality, and singularities in the electronic density of states.<sup>3-5</sup> On the other hand, a completely different interpretation has been established for the defect-induced  $D$  mode at  $\approx 1350 \text{ cm}^{-1}$ . Similar to graphite, the  $D$  mode originates from a double-resonant Raman process involving phonon wave vectors corresponding roughly to the  $K$  point in graphite.<sup>6,7</sup> This interpretation leads to the question of whether the high-energy Raman spectrum in carbon nanotubes is also dominated by processes that allow phonon wave vectors throughout the whole Brillouin zone.

In contrast to graphite, the experimental high-energy mode structure in carbon nanotubes consists of several peaks of different amplitude, the two most intense being separated by  $\approx 20 \text{ cm}^{-1}$ . This peculiar peak structure is not only found in bundled nanotubes but also in measurements on individual tubes.<sup>8,9</sup> In spite of intensive research, the double-peak structure of the high-energy mode has not been understood. Some authors suggested that the different high-energy mode peaks correspond to  $\Gamma$ -point vibrations with different symmetries ( $A_{1(g)}$ ,  $E_{1(g)}$ , and  $E_{2(g)}$ , where the subscript  $g$  refers to armchair and zigzag tubes).<sup>10,11</sup> This is contradicted by polarization-dependent Raman measurements, which show that the  $A_{1(g)}$  phonon modes contribute most to the Raman spectra of nanotubes.<sup>8,12,13</sup> Taking this into account, it was suggested that the two most intense peaks correspond to zone-center longitudinal (LO) and transversal (TO) optical phonon modes with their frequency separation caused by different force constants along and perpendicular to the tube axis.<sup>12,14</sup> However, this explanation is questionable: First, there is no reason for the large splitting ( $20 \text{ cm}^{-1}$ ) between TO and LO modes in general chiral tubes, as the phonon modes do not have any more purely longitudinal and trans-

versal character.<sup>15</sup> Only in achiral tubes are the LO- and TO-phonon modes distinguished, but one of them is forbidden by symmetry. Second, in hydrostatic pressure measurements, TO and LO modes in the uniaxial system should exhibit different pressure derivatives, contrary to what is observed experimentally.<sup>16,17</sup> All attempts for understanding the high-energy modes in carbon nanotubes attribute the observed Raman peaks to  $\Gamma$ -point vibrations that correspond to the optical phonon modes of  $E_{2g}$  symmetry in graphite.

In this paper we propose what we believe is a conceptually different explanation for the high-energy modes, which resolves the present discrepancies in the understanding of the Raman spectra. Our basic idea is that the high-energy peaks of carbon nanotubes do not correspond to a phonon mode with a wave vector  $q \approx 0$ , but instead originate from a double-resonance process with phonon wave vectors  $q > 0$ . The high-energy double-peak structure in general chiral tubes is caused by the two optical phonon branches of  $A_1$  symmetry at the  $\Gamma$  point. Our results do not crucially depend on a splitting at the zone center in contrast to theories which are based on the difference between the so-called LO and TO  $\Gamma$ -point modes. Resonant scattering within different electronic bands leads to additional peaks in the high-energy range. In the double-resonance model the high-energy peaks in individual tubes are predicted to shift slightly with excitation energy. We prove our model by showing experimentally positive and negative excitation-energy-dependent shifts of the high-energy frequencies in bundled single-walled nanotubes. In the range of  $E_{\text{laser}}$  from 2.18 to 3.52 eV, the frequency shift has a different sign for the two largest peaks.

A Raman process is doubly resonant if two of the transitions in the scattering process are real. This condition can always be fulfilled in higher-order scattering with large phonon wave vectors. The apparent breaking of wave-vector conservation might, e.g., be due to impurities or other imperfections in the lattice, a small size of the scattering crystal, or a high optical absorption.<sup>18</sup> The  $D$  mode in the Raman spectra of both graphite and single-walled carbon nanotubes originates from such defect-induced, double-resonant Raman scattering.<sup>6,7</sup> In Fig. 1 we show the electronic band structure of the (11,11) tube with three double-resonant scattering processes. In our example, the incoming photon is absorbed in a resonant transition near the conduction-band minimum, and the excited electron is resonantly scattered within the

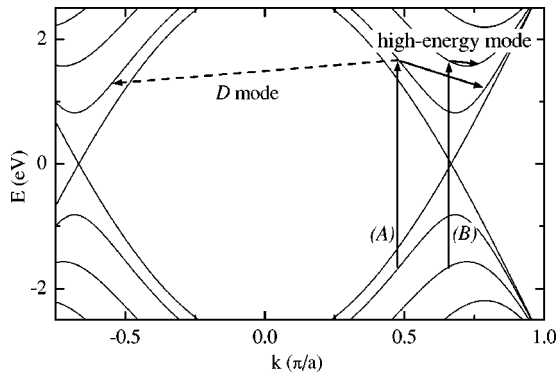


FIG. 1. Electronic band structure of the (11,11) tube. Three double-resonant scattering processes are shown schematically; one leading to the  $D$  mode (dashed arrow) and two leading to the high-energy modes (solid arrows). Processes  $A$  and  $B$  result in different phonon frequencies.

same electronic band. The other two steps of the resonant process, scattering of the electron by a defect and recombination of the electron-hole pair, are not shown in Fig. 1.<sup>6</sup> Resonant scattering of the excited electron across the  $\Gamma$  point (dashed arrow) leads to the  $D$  mode in the Raman spectra.<sup>7</sup> The second possibility for a real transition of the excited electron is scattering across the conduction-band minimum (solid arrows). We find that this process contributes to the Raman spectra as well and leads to the high-energy modes of carbon nanotubes. The phonon mode involved here possesses a small wave vector (as compared to the  $D$ -mode process, but large compared to the wave vector of light) and hence a frequency near the  $\Gamma$ -point frequency. Two optical branches result in two high-energy Raman peaks. Consequently, we expect that the radial breathing mode also originates from the same double-resonant process. At a given excitation energy, the wave vector and frequency of the phonon depend on the particular electronic band in which the electron is resonantly scattered. For example, in process  $A$  (Fig. 1) the phonon wave vector  $q$  for resonant scattering is larger than in process  $B$ . These two transitions yield Raman peaks at different frequencies. Similar to the  $D$ -mode in nanotubes and graphite, the double-resonance condition changes with the laser wavelength. The electron wave vector at which the incoming (or outgoing) resonance occurs and the phonon wave vector for the second resonance depend on the excitation energy. As is obvious from Fig. 1, with increasing laser energy the phonon wave vector fulfilling the double-resonance condition becomes larger. The frequency of the Raman peaks then shifts with excitation energy according to the dispersion of the phonon branches near the  $\Gamma$  point.

We explicitly calculated the high-energy Raman spectra of single-walled carbon nanotubes from the cross section for defect-induced, double-resonant Raman scattering.<sup>18,7</sup> We chose the incoming and outgoing light to be polarized parallel to the tube axis. We obtained the electron dispersion by the symmetry-based tight-binding approximation with an overlap integral  $\gamma_0 = 2.9$  eV.<sup>19</sup> For the phonon dispersion we used a model dispersion adapted from graphite; see inset of Fig. 2.<sup>20</sup> The phonon branches were degenerate at the  $\Gamma$  point; a splitting does not essentially alter our results. As a

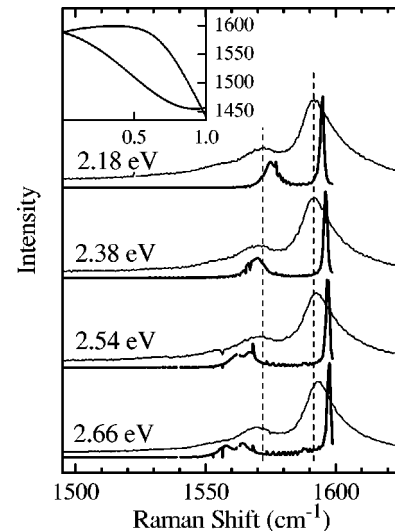


FIG. 2. Experimental (upper curves) and calculated (lower curves) high-energy Raman spectra for excitation energies in the visible. The separation between the peaks increases with increasing laser energy in both experimental and calculated spectra. The inset shows the phonon dispersion used in the calculations. The phonon wave vector  $q$  is given in units of  $\pi/a_0$ ; the phonon frequency is given in  $\text{cm}^{-1}$ .

first approximation, we assume the phonon dispersion near the  $\Gamma$  point (for  $q \in [0, \pi/a_0]$ , where  $a_0$  is the length of the graphite lattice vectors) to be independent of the tube chirality. Our samples in Raman scattering were single-walled nanotubes with a mean diameter of 1.45 nm. The tubes were excited with an  $\text{Ar}^+ \text{Kr}^+$  laser; the light was dispersed by a triple monochromator, and detected with a charge-coupled device.

In Fig. 2 we show our experimental high-energy Raman spectra and the calculation for the (15,6) tube. Double-resonant Raman scattering describes the essential features of the measured spectra surprisingly well. In particular, we find the strongest peak at  $1597 \text{ cm}^{-1}$  above the  $\Gamma$  point frequency ( $1588 \text{ cm}^{-1}$  in our dispersion, like in graphite) and a second, less intense peak at  $1575 \text{ cm}^{-1}$ . The magnitude of the splitting  $\approx 20 \text{ cm}^{-1}$  as well as the absolute peak positions are in excellent agreement with experiments. The relative amplitude of the two peaks is also similar to the ratio found in the experimental spectra. The crucial point, when comparing the spectra at different excitation energies, is that the Raman peaks shift both in experiment and in our calculation, as predicted. The experimental frequency of the upper peak increases ( $3.5 \text{ cm}^{-1}/\text{eV}$ ), whereas the frequency of the lower peak decreases with increasing excitation energy ( $-1.7 \text{ cm}^{-1}/\text{eV}$ ). Within our model, the frequency shift and the relative position of the peaks follow (in this range of laser wavelength and for this tube) from the phonon dispersion. Because of the weak overbending in the upper phonon branch (see the inset of Fig. 2), the Raman peak at  $1597 \text{ cm}^{-1}$  is at higher frequency than the  $\Gamma$  point frequency. The overbending leads to a positive shift with excitation energy of the peak at  $1597 \text{ cm}^{-1}$ ; accordingly the peak at  $1575 \text{ cm}^{-1}$  shifts to lower frequency with increasing

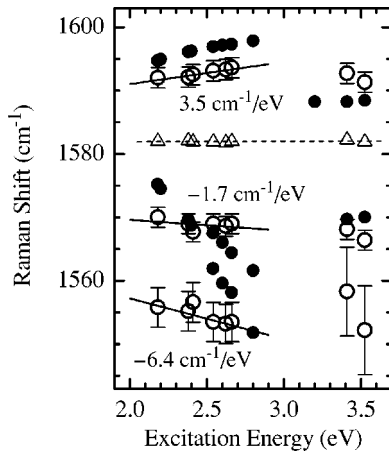


FIG. 3. Frequency of the high-energy Raman peaks as a function of laser excitation energy. Experimental and calculated values are given by open and closed symbols, respectively. The lines are linear fits to the experimental data from  $E_{\text{laser}} = 2.18$  to  $2.66$  eV. Open triangles are experimental data of graphite, where the frequency is clearly independent of the excitation energy.

laser energy. Because of the overbending, the phonon density of states near the  $\Gamma$  point is particularly large for the upper branch. Therefore, the intensity of the upper peak is higher than the intensity of the lower one, as found experimentally.

In the spectra calculated for  $2.54$  and  $2.66$  eV, the peak at  $1560$   $\text{cm}^{-1}$  appears to split. In fact, a double-peak structure is expected for both peaks at each laser energy, because in the (15,6) tube two electronic bands dominate the spectra. The double-resonant process occurs for both bands at slightly different phonon wave vectors. Because the bands are rather close at their minimum, the different contributions to the Raman signal are only resolved at higher laser energies.

So far we have discussed excitation energies involving the same electronic bands. The phonon wave vector in such a double-resonance process continuously increases with increasing laser energy. The excitation-energy dependence of the peaks then reflects only the phonon dispersion near the  $\Gamma$  point. For even larger laser energies, the next higher optical transition can be reached, which again occurs close to the band minimum. The corresponding double-resonant phonon wave vectors are small; the Raman frequencies are expected quite close to the  $\Gamma$ -point frequencies. These contributions dominate the spectra because of the high density of electronic states near the conduction band minimum, an effect which was also seen in the calculated  $D$ -mode intensity.<sup>7</sup> In Fig. 3 we show the excitation-energy dependence of the high-energy modes for laser energies up to  $3.52$  eV. The experimental and calculated Raman frequencies are given by open and closed symbols, respectively. It is clearly seen that the continuous shift of the peaks is interrupted at  $E_{\text{laser}} = 3$  eV. Above, the Raman signal originates from a scattering process close to the minimum of the next higher conduction band. We calculated the high-energy Raman spectra for several chiral tubes with diameters of  $\approx 1.4$  nm and obtained results similar to those for the (15,6) tube. The peaks of different tubes are at different frequencies, which leads to

a broadening of the peaks in bulk samples compared with individual tubes. When averaging over several tubes, we found the frequency shift of the highest peak to differ only slightly from that of the single tube. The frequencies of the lower peaks scatter within a broader range leading to a reduced average frequency shift.<sup>21</sup> The laser energy at which the next electronic band is reached is in general different for semiconducting and metallic tubes. When the laser energy matches the van Hove singularities in the joint density of states, the Raman intensity is particularly large, and the calculated line shapes resemble those of metallic spectra. The spectra of bulk samples are thus determined by a convolution of the electronic density of states and the double-resonant process.

For the  $D$  mode in graphite and carbon nanotubes a difference between the frequencies in Stokes and anti-Stokes Raman spectra followed from the double-resonance model. A similar behavior is expected for the high-energy modes, because the double-resonant phonon wave vector is larger in anti-Stokes scattering than in Stokes scattering. Then the position of the peak at  $\approx 1575$   $\text{cm}^{-1}$  will be at lower frequency in anti-Stokes scattering than in Stokes scattering. In contrast, the difference between Stokes and anti-Stokes spectra for the  $1597$ - $\text{cm}^{-1}$  peak is sensitive to the overbending in the phonon dispersion. Depending on the phonon wave vector at which the maximum frequency occurs, the upper peak is at higher or lower frequency in anti-Stokes spectra. With increasing excitation energy, in anti-Stokes scattering the next optical transition is reached with an outgoing resonance at smaller laser energy than in Stokes scattering. Therefore, the two high-energy peaks might be well separated in Stokes scattering (as in Fig. 2), but close together and broad in anti-Stokes scattering at the same excitation energy. Anti-Stokes Raman spectra have so far been reported only for bulk samples.<sup>22,23</sup> For particular laser energies these experiments indeed show Stokes and anti-Stokes spectra quite different in shape. As a consequence of double-resonant Raman scattering, also we predict a similar behavior for individual nanotubes.

The relative intensities of the  $D$  mode and the high-energy mode in first-order scattering are, in contrast to graphite, not determined by the number of defects but by the chirality of the tube. This is supported by experiments on isolated tubes, which show a strong variation of the intensity ratio when investigating different tubes.<sup>8,9</sup>

Corresponding to the high-energy mode, the radial breathing mode is also expected to originate from a double-resonant Raman process. On the other hand, the slope of the dispersion of the radial breathing mode is nearly zero close to the  $\Gamma$  point; thus the excitation-energy dependence of the Raman frequency is predicted to be small.

In conclusion, we showed that the high-energy modes in the Raman spectra of carbon nanotubes originate from a defect-induced, double-resonant Raman process revising the origin of these modes. The Raman peaks do not originate from the  $\Gamma$ -point vibrations, as is usual in first-order scattering, but from phonons with large wave vectors. This explains why the largest high-energy peak in the Raman spectra occurs at higher frequency than the  $\Gamma$ -point mode in graphite.

The peculiar double-peak structure is due to scattering by the two optical phonons with  $A_1$  symmetry at the  $\Gamma$  point. The double-resonance model implies positive and negative excitation-energy dependences of the Raman frequency, which we confirmed experimentally.

We thank P. Bernier and C. Journet for providing us with the samples, and appreciate discussions with M. Damnjanović about the phonon dispersion. This work was supported by the Deutsche Forschungsgemeinschaft under Grant No. Th 662/8-1.

- 
- <sup>1</sup>J. Kürti *et al.*, Phys. Rev. B **58**, R8869 (1998).  
<sup>2</sup>M. Milnera *et al.*, Phys. Rev. Lett. **84**, 1324 (2000).  
<sup>3</sup>E. Richter *et al.*, Phys. Rev. Lett. **79**, 2738 (1997).  
<sup>4</sup>P.M. Rafailov, *et al.*, Phys. Rev. B **61**, 16 179 (2000).  
<sup>5</sup>A. Jorio *et al.*, Phys. Rev. Lett. **86**, 1118 (2001).  
<sup>6</sup>C. Thomsen *et al.*, Phys. Rev. Lett. **85**, 5214 (2000).  
<sup>7</sup>J. Maultzsch *et al.*, Phys. Rev. B **64**, 121407 (2001).  
<sup>8</sup>G.S. Duesberg *et al.*, Phys. Rev. Lett. **85**, 5436 (2000).  
<sup>9</sup>M.A. Pimenta *et al.*, Phys. Rev. B **64**, 041401 (2001).  
<sup>10</sup>A.M. Rao *et al.*, Science **275**, 187 (1997).  
<sup>11</sup>R. Saito *et al.*, Phys. Rev. B **57**, 4145 (1998).  
<sup>12</sup>A. Jorio *et al.*, Phys. Rev. Lett. **85**, 2617 (2000).  
<sup>13</sup>S. Reich *et al.*, Phys. Rev. B **63**, 041401 (2001).  
<sup>14</sup>R. Saito *et al.*, Phys. Rev. B **64**, 085312 (2001).  
<sup>15</sup>S. Reich *et al.*, Phys. Rev. B **64**, 195416 (2001).  
<sup>16</sup>S. Reich *et al.*, in *Proceedings of the XV International Winter-school on the Electronic Properties of Novel Materials*, edited by H. Kuzmany, J. Fink, M. Mehring, and S. Roth (AIP, Melville, NY, 2001), p. 388.  
<sup>17</sup>S. Reich *et al.*, Phys. Rev. B **61**, R13389 (2000).  
<sup>18</sup>R. M. Martin and L. M. Falicov, in *Light Scattering in Solids I: Introductory Concepts*, 2nd ed., edited by M. Cardona, Topics in Applied Physics, Vol. 8 (Springer-Verlag, Berlin, 1983), p. 79.  
<sup>19</sup>M. Damnjanović *et al.*, J. Phys. A **33**, 6561 (2000).  
<sup>20</sup>D. Sánchez-Portal *et al.*, Phys. Rev. B **59**, 12 678 (1999).  
<sup>21</sup>As a first and simple approximation, we averaged the peak frequencies of seven individual tubes [(15,6), (16,4), (17,2), (15,5), (13,7), (14,7), (12,8)] for excitation energies between 2.18 and 2.66 eV. Indeed, we obtained a 2–3 times smaller average frequency shift for the two lower peaks, while the average shift of the highest peak remains almost the same as for the individual tube.  
<sup>22</sup>S.D.M. Brown *et al.*, Phys. Rev. B **61**, R5137 (2000).  
<sup>23</sup>K. Kneipp *et al.*, Phys. Rev. Lett. **84**, 3470 (2000).